Atmospheric Formation of OH Radicals and H_2O_2 from Alkene Ozonolysis under Humid Conditions

Josep M. Anglada,*[a] Philippe Aplincourt,[b] Josep M. Bofill,[c] and Dieter Cremer[d]

KEYWORDS:

ab initio calculations · atmospheric chemistry · OH formation · radicals · reaction mechanisms

Detailed mechanistic knowledge about the formation of OH radicals and H_2O_2 in alkene – ozone reactions is of enormous interest for tropospheric chemistry, since these molecules are among the most important oxidants in the atmosphere.[1] Hydroxyl radicals oxidize many gaseous trace compounds rapidly and, accordingly, their concentration determines the atmospheric lifetimes of many compounds. Therefore, OH radicals play a key role for the chemistry of the polluted atmosphere.[2] H_2O_2 contributes to acid precipitation by the conversion of SO_2 to H_2SO_4[3] and it is also known to damage trees and plants.[4, 5]

An important source for OH radicals during daytime represents the photolysis of ozone. During nighttime, OH radicals are most likely generated by reactions between NO_3 and aldehydes, or NO_3 and alkenes followed by a reaction with O_2. In recent years, convincing experimental evidence has been collected to confirm the gas phase formation of OH radicals in the ozonolysis of alkenes,[6–9, 11–20, 38] both during day- and nighttime. After early controversies concerning the question how hydroxyl radicals are formed from the alkene – ozone reaction,[10, 11] recent reports on the direct observation of OH radicals provide evidence that OH radicals are produced in the alkene ozonolysis.[12, 13, 19, 20] Quantum chemical investigations have provided convincing evidence that confirm and clarify the mechanism leading to radical formation.[24–29] The process is highly efficient, in particular for internal alkenes,[14, 16, 26, 27] and hence this source of OH radicals competes with the photolysis of ozone in the daytime and with reactions initiated by NO_3 at night.[9]

On the other hand, it is well known that hydrogen peroxide is formed in the atmosphere through recombination of two HO_2 radicals,[1] but recent experimental evidence indicates that the reaction of ozone with alkenes produces H_2O_2 in a mechanism which involves water vapor but no HO_2 radicals.[41–45]

Hence, alkene ozonolysis plays an important role to explain the formation of both OH radicals and H_2O_2 from anthropogenic and biogenic alkenes in urban and rural areas[21, 22] as well as in indoor air.[23] This reaction is initiated by the addition of ozone to the double bond of the alkene and the formation of a primary ozonide (POZ; 1,2,3-trioxolane), which is then cleaved to give a carbonyl oxide (Criegee intermediate) and a carbonyl compound, Equation (1).

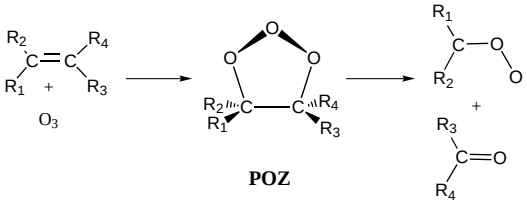

(1)

Carbonyl oxide is formed with an excess of energy and the molecules may undergo unimolecular decomposition or become collisionally stabilized[30–34] so that they can react with other tropospheric species such as water vapor. Vibrationally excited carbonyl oxide molecules can isomerize to dioxirane, which then decomposes into various products in the so-called ester channel[35, 36], Equation (2), or follow, in the case of carbonyl

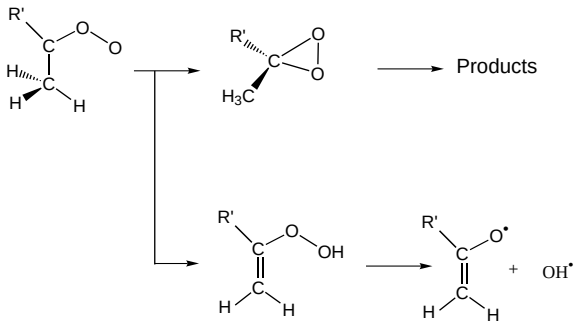

(2)

oxides with hydrogen atoms in the β position, the most favorable hydroperoxide channel, Equation (2).[25–27, 35–37] This path involves a 1,4-hydrogen migration to the terminal oxygen atom of the carbonyl oxide and produces a vibrationally excited unsaturated hydroperoxide, which is cleaved to form OH radicals. Two recent investigations on dimesitylketone *O*-oxide report experimental and theoretical evidence for the OH radical formation mechanism also in solution.[28–29] Another source of OH radicals may arise from a stepwise decomposition mechanism of POZ according to a theoretical study of Anglada et al.[39]

[a] *Dr. J. M. Anglada*
Institut d'Investigacions Químiques i Ambientals de Barcelona
Departament de Química Orgànica Biològica, CSIC
C/Jordi Girona 18, 08034 Barcelona, Catalunya (Spain)
E-mail: anglada@iiqab.csic.es

[b] *Dr. P. Aplincourt*
Laboratoire de Chimie Théorique
UMR CNRS – UHP No 7565, Université Henri Poincaré
BP 239, 54506 Vandoeuvre-les-Nancy Cedex (France)

[c] *Dr. J. M. Bofill*
Departament de Química Orgànica and
Centre de Recerca en Química Teòrica
Universitat de Barcelona
Martí i Franquès 1, 08028 Barcelona, Catalunya (Spain)

[d] *Prof. D. Cremer*
Department of Theoretical Chemistry,
Göteborg University
Reutersgatan 2, 41320 Göteborg (Sweden)

Supporting information for this article is available on the WWW under http://www.chemphyschem.com or from the author.

and an experimental and theoretical investigation by Fenske et al.[47]

In a recent study, Kroll and co-workers[19] pointed out that the OH• yields obtained by direct pressure-dependent measurements in the gas phase ozone – alkene reaction are significantly lower than those determined in scavenger studies. This indicates that additional OH• formation may arise through secondary reactions. In fact, it has been suggested that hydroxyl radicals are also produced by the reaction of carbonyl oxide with water.[35] However, Neeb and Moortgat[16] and Johnson et al.[46] concluded that the OH• yield in alkene ozonolysis experiments is not affected by the presence of H_2O, which is known to react with stabilized carbonyl oxide. Controversies remain therefore important on this question. Furthermore, alkene ozonolysis experiments in absence of H_2O produce only traces of H_2O_2 while the presence of water vapor always leads to the formation of H_2O_2.[44, 45] In this case the proposed mechanism involves the reaction of the corresponding stabilized Criegee intermediate with water.

Following a previous study on the gas-phase reaction mechanism between the parent carbonyl oxide H_2COO and water,[40] we have investigated the reaction between H_2O and substituted carbonyl oxides CH_3HCOO and $(CH_3)_2COO$. First of all, we focused our attention on the processes that lead to the formation of OH radicals. In addition, we considered the processes that may lead to the formation of acetic acid and H_2O on the one hand and to the aldehydes CH_3HCO and $(CH_3)_2CO+H_2O_2$ on the other. Our theoretical study provides further insight into the reaction mechanism of tropospheric OH• and H_2O_2 production from vibrationally stabilized carbonyl oxides through its reaction with water vapor.

Herein, the different minima in the potential-energy surfaces (PES) are designated by the letter B followed by a number. Different conformers of the same compound are distinguished from each other by addition of primes to the symbol. The transition structures are designated by "TS" followed by the acronyms of the minima they connect. Furthermore, there are some pairs of transition states that describe the same global process, but one of them involves the participation of an additional water molecule. The latter are distinguished from the former by appending the letter c (see, for instance, TSB2-B7 and TSB2-B7c in Figure 2).

Reaction between stabilized Criegee intermediates and water. Formation of α-hydroxy hydroperoxide and OH radicals.

The CCSD(T)/6-311 + G(2d,2p)-level reaction and activation enthalpies and free energies for all the structures considered in the reaction between CH_3HCOO and $(CH_3)_2COO$ with water are listed in Table 1. The corresponding values for H_2COO[40] are also included. Figure 1 schematically gives the energetics of the reaction between CH_3HCOO and H_2O. Calculated values, $\Delta H(298)$, are used to facilitate comparison with experimental data. Part a of the mechanism involves *syn*-methylcarbonyl oxide and part b involves *anti*-methylcarbonyl oxide as reaction partner for water. In part a, the H_2O molecule can react with β-hydrogen atoms in *syn* position, which corresponds also to the situation encountered for $(CH_3)_2COO$. In part b, the H_2O molecule reacts with an α-hydrogen atom in the *syn* position similar to the case of H_2COO.[40]

Our calculations reveal that in both cases the reaction is initiated by the formation of hydrogen-bonded complexes **B1** or **B1′** (7.7 and 8.1 kcal mol^{-1} more stable than reactants, Figure 1) which then can react in the following two different ways.

One reaction possibility involves transition states **TSB1-B2** or **TSB1′-B2′** and produces α-hydroxy hydroperoxide **B2**(= **B2′**). The two reactions can be considered as (symmetry-allowed) 1,3-dipolar additions of water to carbonyl oxide. The activation enthalpies are just 13.4 (part a) and 7.5 kcal mol^{-1} (part b, Figure 1, Table 1). They are considerably smaller than the corresponding barriers for dioxirane formation (23.4 and 15.5 kcal mol^{-1}) or H migration (17.4 and 31.0 kcal mol^{-1}[24–26]). Adduct **B2/B2′** is formed with an excess of enthalpy of 43.4 and 40.5 kcal mol^{-1}, respectively, which is sufficient to cleave its peroxide bond to produce radicals OH• and $CH_3HC(O•)OH$ (**B5**).

A second reaction possibility involves **TSB1-B3** and **TSB1′-B4** and corresponds to a water-catalyzed H migration (see Equation (2)), which also leads to the formation of OH radicals. This possibility was originally proposed by Niki et al.[35] and Martinez and Herron[36–37] and studied by Cremer et al.[25–27] by means of

Table 1. *CCSD(T)/6-311 + G(2d,2p) reaction and activation enthalpies and free energies [kcal mol^{-1}] for the reaction between* syn-CH_3HCOO, $(CH_3)_2COO$, anti-CH_3HCOO *or* H_2COO, *and* H_2O.[a]

Structures	Part a, Carbonyl oxide (R, R′) CH_3, H		CH_3, CH_3		Structures	Part b, Carbonyl oxide (R, R′) H, CH_3		H, H	
	ΔH	ΔG	ΔH	ΔG		ΔH	ΔG	ΔH	ΔG
RR′COO + H_2O	0.0	0.0	0.0	0.0	RR′COO + H_2O	0.0	0.0	0.0	0.0
B1 (Complex)[b]	−7.6	1.1	−8.9	−0.4	**B1′** (Complex)[b]	−8.1	0.8	−7.0	1.9
	(−6.7)	(2.0)	(−7.8)	(0.7)		(−7.0)	(1.9)	(−6.0)	(2.9)
TSB1-B2	5.8	17.4	4.0	15.8	**TSB1′-B2′**	−0.7	10.9	1.9	13.2
B2	−36.6	−25.4	−34.6	−23.1	**B2′**	−41.1	−29.8	−42.1	−31.4
B5 + OH	2.3	2.1	5.2	5.0	**B5** + OH	−1.2	−1.2	−3.1	−3.6
TSB1-B3	9.2	21.1	10.3	19.8	**TSB1′-B4** + H_2O	9.4	20.3	11.9	22.8
B3 + H_2O	−18.6	−19.0	−16.5	−16.9	**B4** + H_2O + OH	−12.2	23.8	−12.6	−23.5
B6 + H_2O + OH	−1.6	−12.6	−0.2	−10.5					

[a] Geometries were calculated at the B3LYP/6-311 + G(2d,2p) level of theory, vibrational corrections at the B3LYP/6-31G(d,p) level. R and R′ refer to the substituents CH_3 or H in *syn* and *anti* position of the carbonyl oxide. [b] The values in parentheses include BSSE corrections.

  1439-4235/02/03/02 $ 17.50+.50/0 CHEMPHYSCHEM **2002**, No. 2

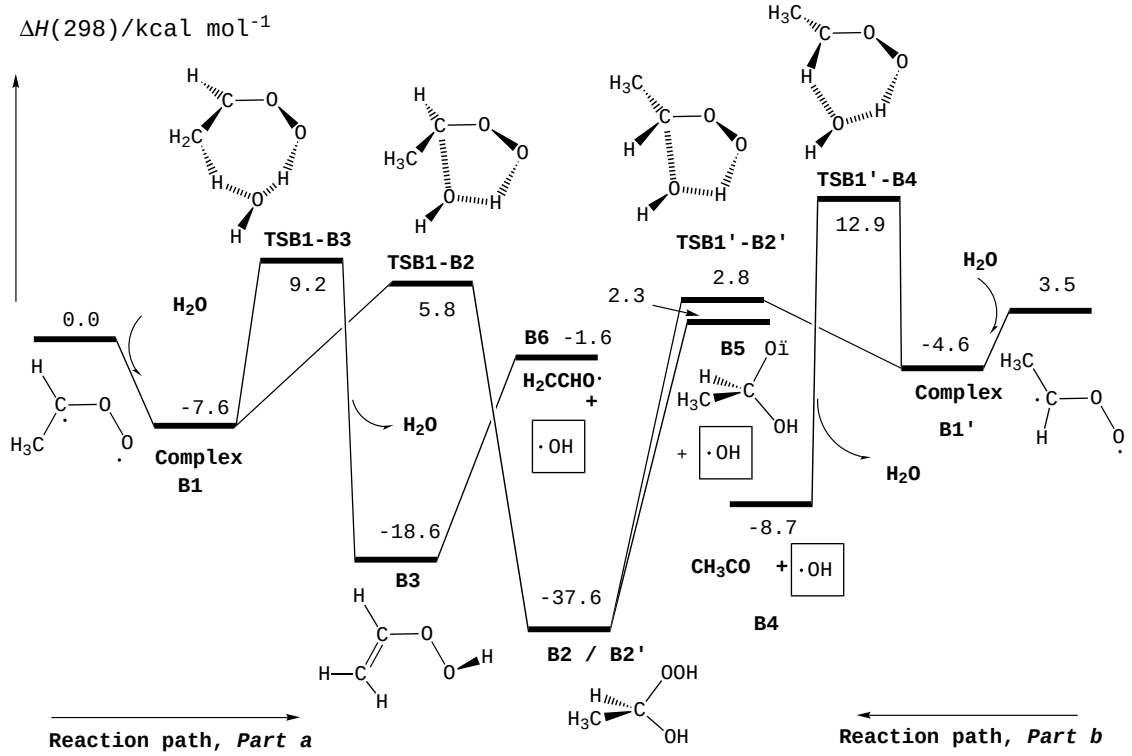

Figure 1. *Schematic enthalpy diagram for the reaction between CH_3HCOO with H_2O. In part a, the CH_3 substituent is in the* syn *position, while in part b, the H substituent is in the* syn *position.*

quantum chemical methods. Water catalysis reduces activation enthalpies (16.8 and 17.6 kcal mol^{-1}, Figure 1) by 8.2 (part a) and 18.0 kcal mol^{-1} (part b), respectively, which however is still 3.4 and 10.1 kcal mol^{-1} higher than the corresponding activation enthalpies for the 1,3-cycloaddition path.

Hence, we conclude that for *anti*-CH_3HCOO cycloaddition of water and formation of **B2/B2′** is the preferred reaction while for the *syn*-CH_3HCOO both cycloaddition and the water-catalyzed H migration can take place in the gas phase where, in all cases, OH radicals are produced. In any case, OH$^{\bullet}$ production is more favorable by 16 – 18 kcal mol^{-1} than dioxirane formation. This underlines the important role of water in carbonyl oxide reactions. Similar results are obtained for the $(CH_3)_2COO$ and H_2COO+H_2O reaction (see Table 1 and ref. [40]) as well as for the reaction between water and the carbonyl oxides generated in isoprene ozonolysis.[55] The three-step mechanism of the reaction between carbonyl oxide and water can be summarized according to Equation (3).

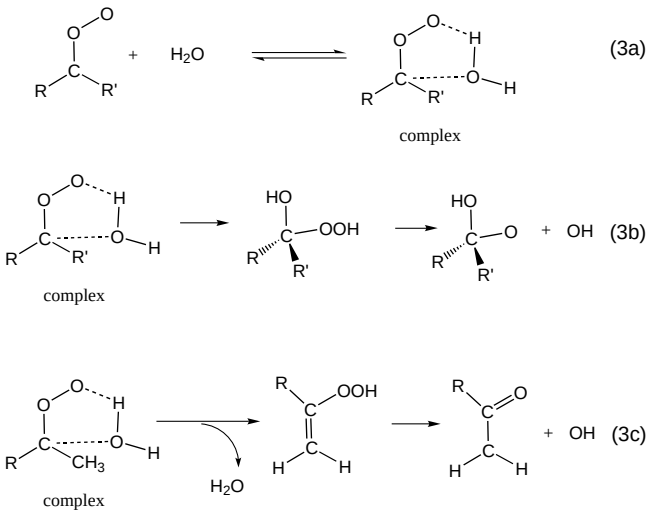

In the first step 3a, a hydrogen-bonded complex is formed; subsequent OH radical formation may then occur in two possible ways: steps 3b and 3c. To determine the competition between processes 3b and 3c, we have computed rate constants utilizing classical transition state theory (Table 2). Although the formation of the water complex (reaction 3a) is exothermic by 7.6 and 8.1 kcal mol^{-1}, the equilibrium between reactants and the product complex is shifted by 80% and more to the side of the reactants because of the entropy change ($\Delta G(298) =$ 0.8 kcal mol^{-1}; except $R = R' = CH_3$: -0.4 kcal mol^{-1}, Table 2). Since the equilibrium (3a) does not affect the branching ratio Γ, the latter is simply calculated as k_{3c}/k, where k is the sum of rate constants k_{3b} and k_{3c}. The data in Table 2 indicate that for substituted carbonyl oxides with β-hydrogen atoms in *syn* positions, the water-catalyzed hydroxyperoxide channel (**TSB1-B3**) plays a minor role (5.2% and 2.6% branching in the case of *syn*-CH_3HCOO and $(CH_3)_2COO$) while for substituted carbonyl oxides with α-H atoms in the *syn* position, the water-catalyzed hydroxyperoxide channel (**TSB1′-B4**) is not active at all. In the literature, estimates for the second-order rate constant of the reaction between H_2COO and H_2O without the formation of an intermediate water complex are given in the range from 1×10^{-15} to 2×10^{-19} cm^3 molecule^{-1} s^{-1}.[56] The corresponding value

Table 2. CCSD(T)/6-311 + G(2d,2p) tunneling parameters κ and rate constants k for the reaction between syn-CH_3HCOO, $(CH_3)_2COO$, anti-CH_3HCOO or H_2COO and H_2O.[a]

		Unimolecular reaction					Bimolecular reaction		
R, R′	κ	k_{3b} [s^{-1}]	κ	k_{3c} [s^{-1}]	$\Gamma = k_{3c}/k$[c]	κ	k [$cm^3 mol^{-1} s^{-1}$]	κ	k [$cm^3 mol^{-1} s^{-1}$]
Part a		**TSB1-B2**		**TSB1-B3**			**TSB1-B2**		**TSB1-B3**
CH_3, H	b	13.128	25.030	0.7232	5.20	b	4.23325×10^{-20}	16.987	1.58282×10^{-21}
CH_3, CH_3	b	16.685	29.261	0.4525	2.64	1.104	7.48640×10^{-19}	16.334	1.02616×10^{-20}
Part b		**TSB1′-B2′**		**TSB1′-B4**			**TSB1′-B2′**		**TSB1′-B4**
H, CH_3	b	4.97475x10^5	3.966	0.2537	–	b	2.54020×10^{-15}	4.068	1.32854×10^{-21}
H, H	b	64757	8.990	0.0553	–	1.152	5.88344×10^{-17}	9.294	4.50534×10^{-23}

[a] Partition functions were calculated at the B3LYP/6-31G(d,p) level of theory. R and R′ refer to the substituents of the carbonyl oxide in the *syn* and *anti* position, respectively. [b] Parameter $\kappa < 1$ and therefore tunneling was not taken into account. [c] Branching ratio (in percent) for the water-catalyzed hydroxyperoxide channel (3c). Parameter k_{3c} is the computed rate constant for 3c while $k = k_{3b} + k_{3c}$ is the total rate constant. No values are given when the branching ratio is negligible.

obtained in this study is 5.88×10^{-17} cm^3 $molecule^{-1}$ s^{-1} (Table 2) and falls into the range of experimental estimates.

Equations (3b) and (3c) lead to different products and therefore should be easily distinguished experimentally. Also, for the channel involving the α-hydroxy hydroperoxide (**B2**) one could check in the presence of D_2O whether an uncatalyzed H migration which yields OH radicals takes place at all beside reaction 3c (yielding OD radicals and HDO).

Unimolecular and water-assisted decomposition of the α-hydroxy hydroperoxide (B2)

Table 1 and Figure 1 have shown that α-hydroxy hydroperoxide (**B2**) is formed with an excess of energy of about 48 kcal mol^{-1} which is sufficient to cleave its peroxide bond and produce **B5** and OH radicals. However, vibrationally excited **B2** can also decompose unimolecularly or become collisionally stabilized and undergo a further bimolecular reaction. Besides **B5** and OH radicals, in the case of $CH_3HC(OH)OOH$, (**B2**), the unimolecular decomposition leads also to CH_3HCO (**B7**) + H_2O_2 and CH_3COOH (**B8**) + H_2O, Equation (4), while for $(CH_3)_2C(OH)OOH$), only the corresponding aldehyde ($(CH_3)_2CO$)+ H_2O_2 is formed, Equation (4).

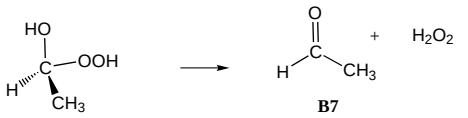

B7 (4a)

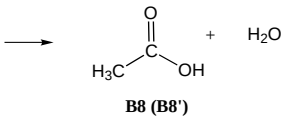

B8 (B8') (4b)

The bimolecular reaction of **B2** with water leads to the same products as the unimolecular decomposition and therefore we name this the water-assisted decomposition of **B2**. The corresponding reaction and activation energies, enthalpies and free energies are included in Table 3, while Figure 2 displays a schematic reaction free-energy profile for $CH_3HC(OH)OOH$.

The unimolecular decomposition of **B2** involves the transition state **TSB2-B7** producing **B7** + H_2O_2 and the transition states **TSB2-B8** and **TSB2′-B8** producing **B8** + H_2O. Table 3 and Figure 2 show clearly that the corresponding activation energies are larger than the energy required for the cleavage of the peroxide bond in **B2** already showed in Table 1 and Figure 1. Thus, the formation of **B5** and OH radicals dominates the reaction mechanism.

For the amount of **B2** that could have been vibrationally stabilized, the bimolecular reaction with water will lead to aldehyde **B7**, H_2O_2, and H_2O involving the transition state **TSB2-B7c**, while the formation of acetic acid (**B8** and **B8′**) plus 2 H_2O may occur through the transition states **TSB2-B8c** and **TSB2-B8′c**.

Looking at the corresponding activation energies, Table 3 and Figure 3 show clearly that, in this case, **B7** and H_2O_2 will be the products formed, since this path is the one with the lowest activation barrier. In the case of $CH_3HC(OH)OOH$, our computed $\Delta H(298)$ and $\Delta G(298)$ values for **TSB2-B7c** are 23.0 and 33.3 kcal mol^{-1} respectively, while the paths which lead to the formation of acetic acid and water have higher energy barriers by about 6 and 11 kcal mol^{-1}. Please note from Table 3 and Figure 2 that there is a catalytic effect of water for **TSB2-B8′c** and **TSB2-B7c** when compared with the unimolecular processes. This water-assisted reaction mechanism enhances the production of H_2O_2 as a result of the reaction of the Criegee intermediates with water, that has been reported experimentally by Sauer et al.[44] and by Winterhalter et al.[45] Moreover, taking into account both the unimolecular and water-assisted decomposition of **B2** and the fact that it is formed with an excess of vibrational energy, one may expect pressure-dependent results. Thus, at low pressures one could expect formation of OH radicals through unimolecular decomposition of **B2** as depicted in Equation (3b). However, in competition with collisional stabilization, the water-assisted decomposition of **B2** will produce H_2O_2 and correspond to Equation (4a) assisted by a water molecule. Finally, it is noteworthy that similar results were obtained for the reaction between H_2O and H_2COO[40] or carbonyl oxides generated in the isoprene ozonolysis.[55]

Conclusions

The results obtained in this work stress the importance of water in the reactions of substituted carbonyl oxides that lead to the

  1439-4235/02/03/02 $ 17.50+.50/0 CHEMPHYSCHEM **2002**, No. 2

Table 3. *Zero point energies [a] (ZPE)*, entropies (*S*), relative energies (*E*), relative enthalpies (*H*), and relative free energies (*G*) for the unimolecular and water-assisted decomposition of RR′C(OH)OOH (**B2**).

Compound	R, R′	*ZPE* [kcal mol^{-1}] B3LYP	*S* [e. u.] B3LYP	ΔE [kcal mol^{-1}] CCSD(T)	ΔH [kcal mol^{-1}] CCSD(T)	ΔG CCSD(T)
			Reactants			
B2 + H_2O	CH_3, H	67.7	120.2	0.0	0.0	0.0
	CH_3, CH_3	84.4	127.0	0.0	0.0	0.0
			Unimolecular decomposition			
TSB2-B7 + H_2O	CH_3, H	63.0	122.9	49.3	44.8	43.9
	CH_3, CH_3	80.1	130.5	46.8	42.7	41.7
TSB2-B8 + H_2O	CH_3, H	63.0	121.8	48.6	44.0	43.5
TSB2′-B8 + H_2O	CH_3, H	62.5	119.0	51.3	45.8	46.1
B5 + OH + H_2O	CH_3, H	61.6	158.3	43.7	38.9	27.5
	CH_3, CH_3	78.9	165.9	43.8	39.6	28.0
			Water-assisted decomposition			
TSB2-B7c[b]	CH_3, H	65.8	85.7	26.2	23.0	33.3
	CH_3, CH_3	82.6	91.6	25.5	22.5	33.0
TSB2-B8c[b]	CH_3, H	65.3	85.0	38.1	34.3	44.9
TSB2-B8′c[b]	CH_3, H	63.5	83.8	34.4	28.8	39.6
			Products			
B7[c] + H_2O_2 + H_2O	CH_3, H	63.6	162.3	14.9	12.0	−0.5
	CH_3, CH_3	80.9	172.9	13.0	10.7	−2.9
B8[c] + 2H_2O	CH_3, H	64.4	158.9	−73.8	−75.7	−87.2
B8′[c] + 2H_2O	CH_3, H	64.2	158.5	−68.6	−70.7	−82.0

[a] *ZPE* scaled by 0.9806 in order to take into account the anharmonic effects.[50] [b] Suffix "**c**" stands for water-assisted decomposition of **B2**. [c] **B7** stands for CH_3CHO or $(CH_3)_2CO$ respectively ; **B8** and **B8′** stands for *syn*- and *anti*-CH_3COOH respectively.

atmospheric production of OH radicals and H_2O_2. Water and carbonyl oxides form relatively stable van der Waals complexes, which are the starting points of the reactions of carbonyl oxides in humid air. The preferred reaction mode is the 1,3-dipolar addition of water to carbonyl oxide yielding α-hydroxy hydroperoxide **B2**, which in view of its excess energy can undergo O—O cleavage to produce OH radicals. The water-catalyzed H migration adds a small percentage (5%) to the OH$^{\bullet}$ production hydroperoxide channel which would be active in the case of substituted carbonyl oxides with H atoms in β position.

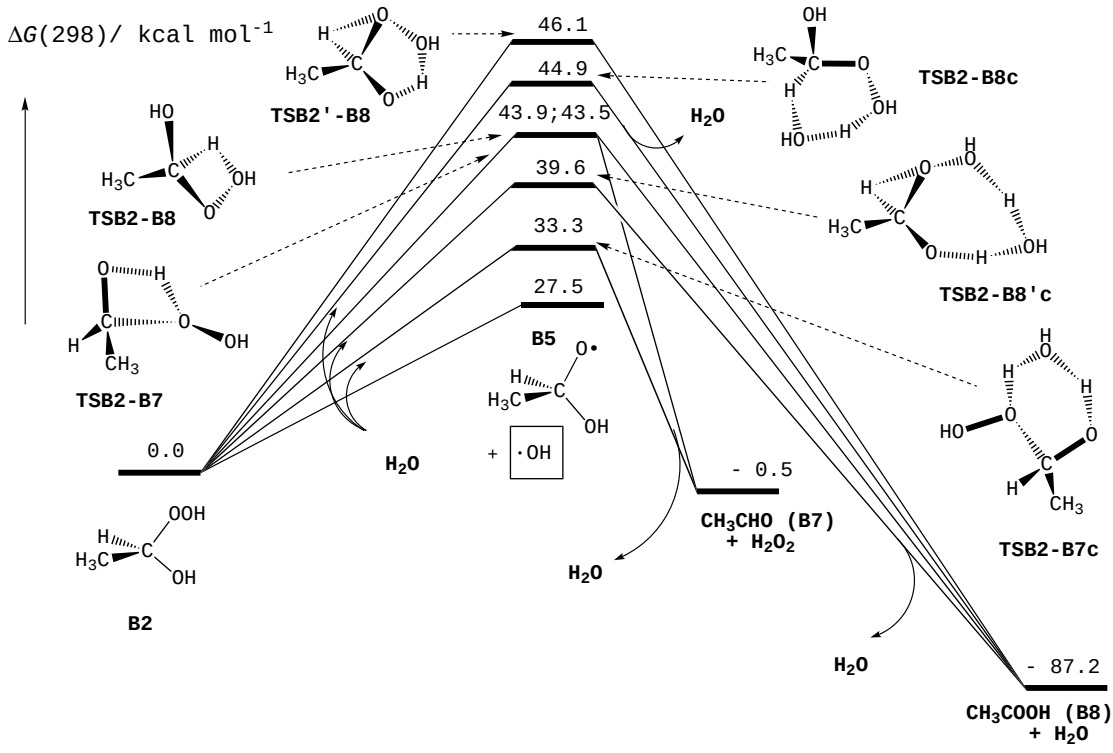

Figure 2. *Schematic free-energy diagram for the unimolecular and water-assisted decomposition of α-hydroxy hydroperoxide.*

Experimentally it should be possible to distinguish the different reaction modes studied. Hence, our investigations provide an important insight into the processes leading to OH radical formation in the polluted atmosphere. For the thermalized α-hydroxy hydroperoxide **B2** our results indicate that its bimolecular reaction with water leads to the formation of the corresponding aldehyde plus H_2O_2.

Computational Methods

We employed density functional theory with the B3LYP hybrid functional[48] to fully optimize the geometries corresponding to minima and saddle points. In a preliminary step, geometries were optimized using the 6-31G(d,p) basis set[49a] and the harmonic vibrational frequencies were calculated to verify the nature of the corresponding stationary points. These calculations were also used to determine the zero-point vibrational energy (ZPE) and the temperature corrections to calculate enthalpies *H* and free energies *G* at $T = 298$ K. In order to take into account the anharmonic effects, the ZPEs were scaled by 0.9806.[50] Moreover, we have carried out intrinsic reaction coordinate (IRC) calculations for each transition state to ensure that the transition states connect reactants and products. In a second step, all stationary points were optimized again by using the more flexible 6-311 + G(2d,2p) basis set[49b] In addition, we have performed single point CCSD(T)/6-311 + G(2d,2p) energy calculations[51] at the B3LYP/6-311 + G(2d,2p) optimized geometries to obtain more reliable energy values. At this level of theory, we corrected also the basis set superposition error (BSSE) in the case of van der Waals complexes using the counterpoise method by Boys and Bernardi.[52] All these calculations were carried out with the Gaussian 94 program package.[53]

For some selected reaction paths, we have also computed the rate constants utilizing classical transition state theory. These rate constants were calculated using CCSD(T)/6-311 + G(2d,2p) energy barriers with partition functions and zero point correction energies obtained at the B3LYP/6-31G(d,p) level of theory. The tunneling correction to the rate constant was calculated by the zero-order approximation to the vibrationally adiabatic PES with zero curvature,[54] where the potential-energy curve is approximated by an unsymmetrical Eckart potential-energy barrier. The Rate program of Truong et al. was used in these calculations.[57]

This research was supported by the Dirección General de Investigación Cinetífica y Técnica (DGICYT, Grants PB98-1240-C02-01 and PB98-1240-C02-02) in Barcelona and by the Swedish Natural Science Research Council (NFR) in Göteborg. P.A. thanks the European Community, Access to Research Infrastructure action of the Improving Human Potential Program for financial support (contract no. HPRI – 1999 – CT – 00071). The calculations described in this work were performed on the supercomputers of the CESCA (Barcelona). We also thank Professor S. Olivella (IIQAB-CSIC) for valuable suggestions.

[1] A. M. Thompson, *Science* **1992**, *256*, 1157 – 1165.
[2] R. P. Wayne, *Chemistry of Atmospheres*, Oxford University Press, Oxford, **2000**.
[3] J. G. Calvert, A. Lazrus, G. L. Kok, B. G. Heikes, J. G. Walega, J. Lind, C. A. Cantrell, *Nature* **1985**, *317*, 27 – 35.
[4] D. Möller, *Atmos. Environ.* **1989**, *23*, 1625 – 1627.
[5] C. N. Hewitt, G. L. Kok, R. Fall, *Nature* **1990**, *344*, 56 – 58.
[6] R. Atkinson, S. M. Aschmann, J. Arey, B. Shorees, *J. Geophys. Res.* **1992**, *97*, 6065 – 6073.
[7] R. Atkinson, S. M. Aschmann, *Environ. Sci. Technol.* **1993**, *27*, 1357 – 1363.
[8] R. Atkinson, E. C. Tuazon, S. M. Aschmann, *Environ. Sci. Technol.* **1995**, *29*, 1860 – 1866.
[9] S. E. Paulson, J. J. Orlando, *Geophys. Res. Lett.* **1996**, *23*, 3727 – 3730.
[10] C. Schaefer, O. Horie, J. N. Crowley, G. K. Moortgat, *Geophys. Res. Lett.* **1997**, *24*, 1611 – 1614.
[11] S. E. Paulson, A. D. Sen, P. Liu, J. D. Fenske, M. J. Fox, *Geophys. Res. Lett.* **1997**, *24*, 3193 – 3196.
[12] T. Pfeiffer, O. Forberich, F. J. Comes, *Chem. Phys. Lett.* **1998**, *298*, 3251 – 3258.
[13] N. Donahue, J. H. Kroll, J. G. Anderson, *Geophys. Res. Lett.* **1998**, *25*, 59 – 62.
[14] S. E. Paulson, M. Y. Chung, A. S. Hasson, *J. Phys. Chem. A* **1999**, *103*, 8127 – 8138.
[15] S. E. Paulson, J. D. Fenske, A. D. Sen, T. W. Callahan, *J. Phys. Chem. A* **1999**, *103*, 2050 – 2059.
[16] P. Neeb, G. K. Moortgat, *J. Phys. Chem. A* **1999**, *103*, 9003 – 9012.
[17] D. Mihelcic, M. Heitlinger, D. Kley, P. Müsgen, A. Volz-Thomas, *Chem. Phys. Lett.* **1999**, *301*, 559 – 564.
[18] A. G. Lewin, D. Johnson, D. W. Price, G. Marston, *Phys. Chem. Chem. Phys.* **2001**, *3*, 1253 – 1261.
[19] J. H. Kroll, J. S. Clarke, N. M. Donahue, J. G. Anderson, K. L. Demerjian, *J. Phys. Chem. A* **2001**, *105*, 1554 – 1560.
[20] J. H. Kroll, J. S. Clarke, N. M. Donahue, J. G. Anderson, K. L. Demerjian, *J. Phys. Chem. A* **2001**, *105*, 4446 – 4457.
[21] J. Hu, D. H. Stedman, *Environ. Sci. Technol. A* **1991**, *25*, 1655 – 1659.
[22] S. Madronich, J. G. Calvert, *J. Geophys. Res.* **1990**, *95*, 5697 – 5715.
[23] C. J. Weschler, H. C. Shields, *Environ. Sci. Technol.* **1996**, *30*, 3250 – 3258.
[24] J. M. Anglada, J. M. Bofill, S. Olivella, A. Solé, *J. Am. Chem. Soc.* **1996**, *118*, 4636 – 4647.
[25] R. Gutbrod, R. N. Schindler, E. Kraka, D. Cremer, *Chem. Phys. Lett.* **1996**, *252*, 221 – 229.
[26] R. Gutbrod, E. Kraka, R. N. Schindler, D. Cremer, *J. Am. Chem. Soc.* **1997**, *119*, 7330 – 7342.
[27] M. Olzmann, E. Kraka, D. Cremer, R. Gutbrod, S. Andersson, *J. Phys. Chem.* **1997**, *101*, 9421 – 9429.
[28] D. Cremer, E. Kraka, C. Sosa, *Chem. Phys. Lett.* **2001**, *337*, 199 – 208.
[29] W. Sander, K. Block, W. Kappert, A. Kirschfeld, S. Muthusamy, K. Schroeder, C. P. Sosa, E. Kraka, D. Cremer, *J. Am. Chem. Soc.* **2001**, *123*, 2618 – 2627.
[30] F. Su, J. G. Calvert, J. H. Shaw, *J. Phys. Chem.* **1980**, *84*, 239 – 246.
[31] O. Horie, G. K. Moortgat, *Atmos. Environ. Part A* **1991**, *25*, 1881 – 1896.
[32] R. Atkinson, *J. Phys. Chem. Ref. Data* **1997**, *26*, 215.
[33] P. Neeb, O. Horie, G. K. Moortgat, *J. Phys. Chem. A* **1998**, *102*, 6778 – 6785.
[34] O. Horie, G. K. Mortgat, *Acc. Chem. Res.* **1998**, *31*, 387 – 396.
[35] H. Niki, P. D. Maker, C. M. Savage, L. P. Breitenbach, M. D. Hurley, *J. Phys. Chem.* **1987**, *91*, 941 – 946.
[36] R. I. Martinez, J. T. Herron, *J. Phys. Chem.* **1987**, *91*, 946 – 953.
[37] R. I. Martinez, J. T. Herron, *J. Phys. Chem.* **1988**, *92*, 4644 – 4648.
[38] S. E. Paulson, R. C. Flagan, J. H. Seinfeld, *Int. J. Chem. Kinet.* **1992**, *24*, 103 – 125.
[39] J. M. Anglada, R. Crehuet, J. M. Bofill, *Chem. Eur. J.* **1999**, *5*, 1809 – 1822.
[40] R. Crehuet, J. M. Anglada, J. M. Bofill, *Chem. Eur. J.* **2001**, *7*, 2227 – 2235.
[41] K. H. Becker, K. J. Brockmann, J. Bechara, *Nature* **1990**, *346*, 256 – 258.
[42] K. H. Becker, J. Bechara, K. J. Brockmann, *Atmos. Environ. Part A* **1993**, *27*, 57 – 61.
[43] C. N. Hewitt, G. L. Kok, *J. Atmos. Chem.* **1991**, *12*, 181 – 194.
[44] F. Sauer, C. Schäfer, P. Neeb, O. Horie, G. K. Moortgat, *Atmos. Environ.* **1999**, *33*, 229 – 241.
[45] R. Winterhalter, P. Neeb, D. Grossmann, A. Kolloff, O. Horie, G. K. Moortgat, *J. Atmos. Chem.* **2000**, *35*, 165 – 197.
[46] D. Johnson, A. G. Lewin, G. Marston, *J. Phys. Chem. A* **2001**, *105*, 2933 – 2935.
[47] J. D. Fenske, A. L. Hasson, S. E. Paulson, K. T. Kuwata, A. Ho, K.N Houk, *J. Phys. Chem. A* **2000**, *104*, 7821 – 7833.
[48] A. D. Becke, *J. Chem. Phys.* **1993**, *98*, 5648.
[49] a) P. C. Hariharan, J. A. Pople, *Theor. Chim. Acta* **1973**, *28*, 213; b) R. Krishnan, J. S. Binkley, R. Seeger, J. A. Pople, *J. Chem. Phys.* **1980**, *72*, 650.
[50] A. P. Scott, L. Radom, *J. Phys. Chem.* **1996**, *100*, 16502 – 16513.

[51] a) J. Cizek, *Adv. Chem. Phys.* **1969**, *14*, 35; b) R. J. Barlett, *J. Phys. Chem.* **1989**, *93*, 1963; c) K. Raghavachari, G. W. Trucks, J. A. Pople, M. Head-Gordon, *Chem. Phys. Lett.* **1989**, *157*, 479.
[52] S. F. Boys, F. Bernardi, *Mol. Phys.* **1970**, *19*, 553.
[53] Gaussian 94 (Revision A.5), M. J. Frisch, G. W. Trucks, H. B. Schlegel, P. M. W. Gill, B. G. Johnson, M. A. Robb, J. R. Cheeseman, T.Keith, G. A. Petersson, J. A. Montgomery, K. Raghavachari, M. A. Al-Laham, V. G. Zakrzewski, J. V. Ortiz, J. B. Foresman, J. Cioslowski, B. B. Stefanov, A. Nanayakkara, M. Challacombe, C. Y. Peng, P. Y. Ayala, W. Chen, M. W. Wong, J. L. Andres, E. S. Replogle, R. Gomperts, R. L. Martin, D. J. Fox, J. S. Binkley, D. J. Defrees, J. Baker, J. P. Stewart, M. Head-Gordon, C. Gonzalez, J. A. Pople, Gaussian, Inc., Pittsburgh, PA, **1995**.
[54] T. N. Truong, D. G. Truhlar, *J. Chem. Phys.* **1990**, *93*, 1761.
[55] P. Aplincourt, J. M. Anglada, unpublished results.
[56] J. D. Fenske, A. L. Hasson, A. W. Ho, S. E. Paulson, *J. Phys. Chem. A* **2000**, *104*, 9921 – 9932.
[57] http://therate.hec.utah.edu/

Received: June 1, 2001 [Z238]
Revised: September 17, 2001

Water Activity in Aqueous Solutions of Homogeneous Electrolytes: The Effect of Ions on the Structure of Water

Edward Dutkiewicz* and Anna Jakubowska[a]

KEYWORDS:

aldehyde hydration · salt effect · structure – activity relationships · UV/Vis spectroscopy · water chemistry

The degree of water ordering around particular electrolyte ions has been studied many times by different methods, however the results of the studies have not always been consistent,[1–10] which can be explained by the lack of a definite structural description of water.

In this work, an attempt was made at an estimation of the degree of water structure ordering around ions of particular electrolytes on the basis of the determination of water activity a_W, defined as a product of the activity coefficient f_W and water concentration c_W: $a_W = f_W c_W$. The water activity was determined by the method of hydration of aldehydes[11–13] in aqueous solutions of the electrolytes NaCl, KCl, $NaClO_4$, NH_4ClO_4 and $Mg(ClO_4)_2$ as a function of their concentrations.

[a] *Prof. E. Dutkiewicz, Dr. A. Jakubowska*
Department of Physical Chemistry
Adam Mickiewicz University
ul. Grunwaldzka 6, 60-780 Poznań (Poland)
Fax: (+48) 61-8658008
E-mail: edutkiew@amu.edu.pl

The results of measurements performed at $24.5 \pm 0.1\,^{\circ}C$ are collected in Table 1. The measurements were repeated many times, and each time similar values (within the experimental error) of the water activity for a given electrolyte were obtained. The repeatability varies within ± 0.01, however, we have given the values with three decimal figures to illustrate the repeatable tendency of changes in $a_W = f([\text{electrolyte}])$. Table 1 also gives the activity coefficients of water a_W/c_W calculated from the known densities of the solutions.[14] For the solutions of chlorides and sodium perchlorate, the electrolyte concentration dependencies of a_W and a_W/c_W are linear. The slopes of these lines provide information about the electrolytes' effect on water activity, and the electrolytes can be ordered $NaClO_4 > NaCl > KCl$ according to a greater decrease in a_W. Analysis of the electrolyte influence on the activity coefficient a_W/c_W proved that only NaCl causes a decrease in a_W/c_W, whereas $NaClO_4$ and KCl cause it to increase (Figure 1).

Table 1. *Values of the water activity and the water activity coefficients as a function of electrolyte concentration*

Electrolyte	Concentration		Water activity	Water activity coefficients
	c [mol dm^{-3}]	m [mol kg^{-1}]	a_W	a_W/c_W
NaCl	0.0	0.000	1.000	0.01804
	0.5	0.505	0.984	0.01788
	1.0	1.018	0.979	0.01790
	1.5	1.551	0.950	0.01768
	2.0	2.080	0.929	0.01739
KCl	0.0	0.000	1.000	0.018036
	0.5	0.508	0.986	0.018039
	1.5	1.570	0.958	0.018069
	2.0	2.130	0.945	0.018131
$NaClO_4$	0.0	0.000	1.000	0.01804
	0.5	0.517	0.978	0.01819
	1.0	1.063	0.955	0.01827
	1.5	1.641	0.934	0.01839
	2.0	2.265	0.910	0.01854
NH_4ClO_4	0.00	0.000	1.000	0.01804
	0.25	0.254	0.975	0.01781
	0.50	0.515	0.954	0.01768
	0.75	0.780	0.942	0.01763
	1.00	1.060	0.934	0.01782
$Mg(ClO_4)_2$	0.000	0.000	1.000	0.0180
	0.125	0.127	1.004	0.0183
	0.250	0.256	1.002	0.0185
	0.375	0.388	0.959	0.0179
	0.500	0.523	0.928	0.0175
	1.000	1.097	0.854	0.0169
	1.500	1.751	0.790	0.0166

The activity coefficient reflects the character and strength of intermolecular interactions in the system, that is a decreasing activity coefficient indicates increasing interactions and vice versa. Therefore, the behaviour of a_W/c_W as a function of the molal concentration of the electrolyte provides information on the influence of a given electrolyte on water structure. In previous work,[15–17] it was assumed that if the slopes of the straight-line relations $a_W/c_W = f([\text{electrolyte}])$ is positive the electrolyte disrupts the water structure and if it is negative the electrolyte tends to induce water structure ordering.